System and component modelling of a low temperature solar thermal energy conversion cycle

Shadreck M Situmbeko

Freddie L Inambao

University of KwaZulu-Natal, Howard College, Mechanical Engineering, Durban, South Africa

Abstract

Solar thermal energy (STE) technology refers to the conversion of solar energy to readily usable energy forms. The most important component of a STE technology is the collectors; these absorb the shorter wavelength solar energy (400-700nm) and convert it into usable, longer wavelength (about 10 times as long) heat energy. Depending on the quality (temperature and intensity) of the resulting thermal energy, further conversions to other energy forms such as electrical power may follow. Currently some high temperature STE technologies for electricity production have attained technical maturity; technologies such as parabolic dish (commercially available), parabolic trough and power tower are only hindered by unfavourable market factors including high maintenance and operating costs. Low temperature STEs have so far been restricted to water and space heating; however, owing to their lower running costs and almost maintenance free operation, although operating at lower efficiencies, may hold a key to future wider usage of solar energy. Low temperature STE conversion technology typically uses flat plate and low concentrating collectors such as parabolic troughs to harness solar energy for conversion to mechanical and/or electrical energy. These collector systems are relatively cheaper, simpler in construction and easier to operate due to the absence of complex solar tracking equipment. Low temperature STEs operate within temperatures ranges below 300oC. This research work is geared towards developing feasible low temperature STE conversion technology for electrical power generation. Preliminary small-scale concept plants have been designed at 500Wp and 10KWp. Mathematical models of the plant systems have been developed and simulated on the EES (Engineering Equation Solver) platform. Fourteen candidate working fluids and three cycle configurations have been analysed with the models. The analyses included a logic model selector through which an optimal conversion cycle configuration and working fluid mix was established. This was followed by detailed plant component modelling; the detailed component model for the solar field was completed and was based on 2-dimensional segmented thermal network, heat transfer and thermo fluid dynamics analyses. Input data such as solar insolation, ambient temperature and wind speed were obtained from the national meteorology databases. Detailed models of the other cycle components are to follow in next stage of the research. This paper presents findings of the system and solar field component.

Keywords: low temperature solar thermal energy, mathematical model, EEES computer simulations, working fluids, cycle configuration, component and system models

1. Introduction

Most naturally occurring energies such as light energy from the sun, chemical energy in fossil and biomass fuels, mechanical energy in hydro-streams of rivers and oceans, in tidal waves, and in wind etc., thermal energy in geothermal resources, and nuclear energy in nuclear fuels are present not in a readily usable form and sometimes presents a technical burden if an attempt is made to transport it in its natural form. Energy conversion systems allow us to transform the natural energy to conveniently usable, storable and transportable forms. This paper looks at the conversion of low temperature solar thermal energy to electrical energy.

STE technology refers to the conversion of shorter wavelength solar energy (400-700nm) to longer wavelength (about 10 times as long) heat energy. The most important component of a STE technology is the collectors which absorb and convert solar energy into electrical power, for example.

Currently some high temperature solar thermal energy (HTSTE) technologies for electricity production have attained technical maturity and are only hindered by unfavourable market factors including high maintenance and operating costs. Examples of HTSTE technologies include parabolic dish, parabolic trough, and power tower systems (Groenendaal, 2002).

Low temperature solar thermal energy (LTSTE) technologies have so far been restricted to water and space heating with little or no emphasis on power generation. Examples of applications include:

- Evaporation ponds for extraction of sea water salt;
- Concentrating brine solutions in leach mining and removing dissolved solids from waste streams;
- Domestic and process water heating;
- Preheating of ventilation air; and
- Crop drying as in drying of coffee beans and marigolds.

However, owing to their lower running costs and almost maintenance free operation, LTSTE technologies, although operating at lower efficiencies, may hold a key to future wider usage of solar energy.

Current research on LTSTE for power generation include solar thermal organic Rankine cycle, solar thermal Kalina cycle, Solar Chimney and SNAP (Groenendaal, 2002). Figure 1 shows schematic illustrations of the Solar Chimney, SNAP Plants, Organic Rankine and Kalina Cycles.

2. Feasibility study for development of low temperature solar thermal energy

LTSTE conversion technology typically uses flat plate and low concentrating collectors such as parabolic troughs to harness solar energy for conversion to mechanical and/or electrical energy. These collector systems are relatively cheaper, simpler in construction and easier to operate due to the absence of complex solar tracking equipment found in HTSTE systems. LTSTE operate within temperatures ranges below 300°C.

Figures 2 and 3 show two possible experimental setups. The general layout consists of the solar collector, heat exchangers, turbine-generator, pumps and piping. The first concept sketch shows the first experimental setup whereby the heat transfer fluid is pumped through the solar collector where it is heated and is then passed through the evaporator where heat is transferred to the working fluid. In the second experimental setup, as shown in the second concept sketch, the working fluid is directly heated and evaporated by a solar collector. Whereas the first setup has the advantage of eliminating one heat exchanger, the evaporator, and reducing the required piping, it presents other design challenges; for instance the solar collector must have the required corrosion resistance and be able to withstand higher pressures associated with the working fluid.

Preliminary small-scale concept plants have been designed at 500Wp and 10KWp, where the smaller model is intended as a laboratory experiment and the larger as a field experiment. The aim of this laboratory test is to get an insight in the experimental test setup and results recording and analyses as well as to implement any needed improvements. The field experimental setup will involve the 10kWp Low Temperature Solar Energy Conversion Model.

Designing the cycle involves optimally sizing its main components so as to attain the intended output. The main cycle components are the evaporator and condenser heat exchangers, and the turbine and pumps work devices, the solar collectors array and the generator. The other design aspect involves sizing the duct network so as to minimise both pressure and heat losses and determining the quantities

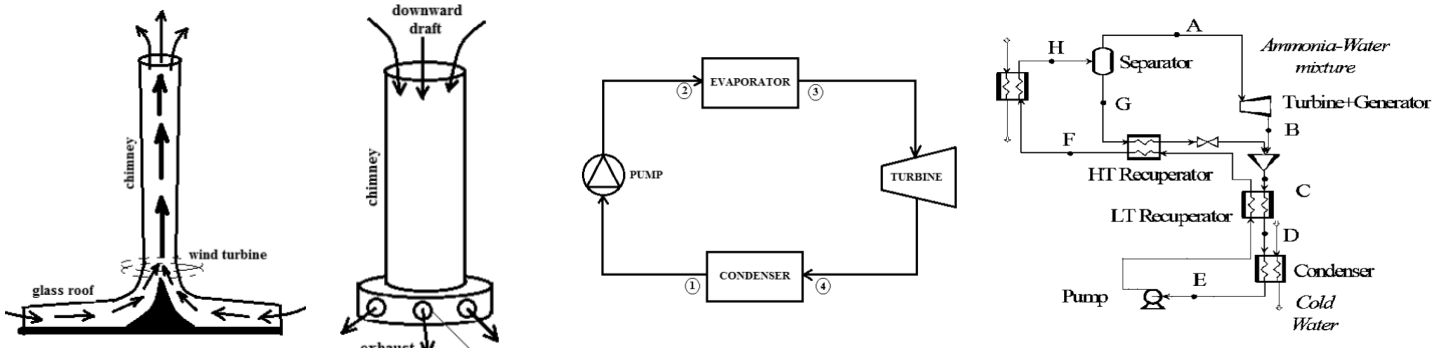

Solar chimney (Schlaich, 1995) *SNAP plant* *Organic Rankine Cycle (montaraventures.com)* *Kalina Cycle (www.eng.usf.edu)*

Figure 1: Examples of low temperature solar thermal energy technologies

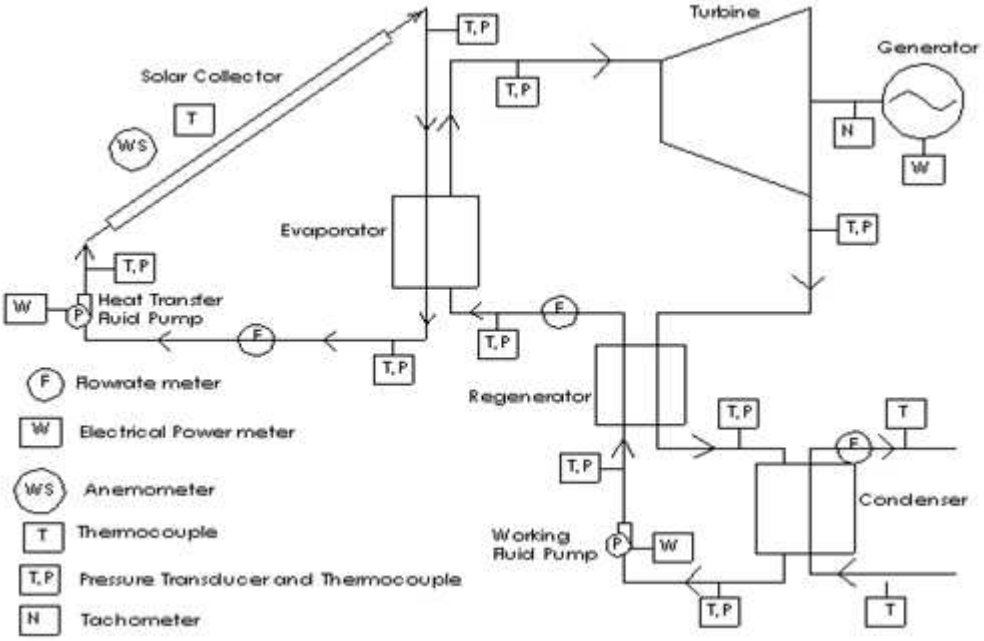

Figure 2: Experimental setup concept 1

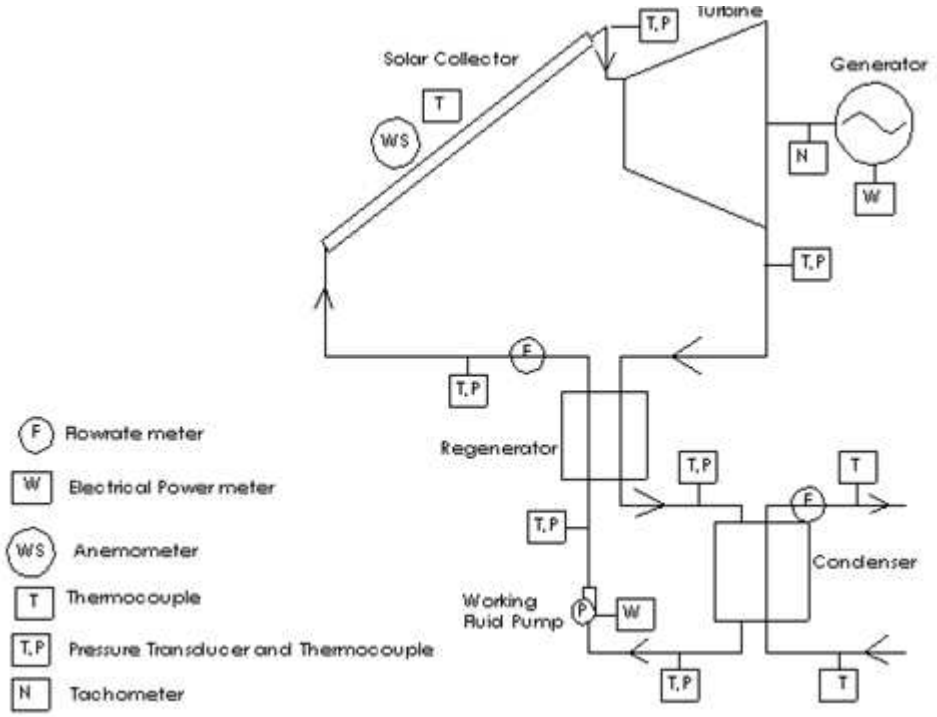

Figure 3: Experimental setup concept 2

of both the working and heat transfer fluids as well as specifying the type of insulation.

The solar field is an important aspect of this design as it involves not only determining the size of the field but also the layout of the solar collectors array.

The preliminary array design is based on the Solardome SA Solar Collector size 1840 x 1650 mm, giving area of 3.04 m^2 (www.solardome.co.za). The efficiencies of flat plate collector from Thermomax Industries (www.thermotechs.com) range from 35 to 50 % for domestic hot water with mean temperature $T_m \approx 55^oC$. Where T_m is the average temperature of fluid in the collector and is given by:

$$Tm = \frac{T_{in} + T_{out}}{2} \quad (1)$$

where T_{in} and T_{out} are respectively the solar collector inlet and outlet temperatures. The range of efficiencies for Rankine cycle operating at low to medium temperatures ranges from 9.9 to 14.1%

(Nishith, 2009). Taking averages the overall system efficiency could be taken as 5.1%. Thus the solar thermal energy available should be about 9.8kW$_{Th}$ for the laboratory model and 196kW$_{Th}$ for the field model. Durban Insolation data averages 4.328 kWh/m^2/day (www.gaisma.com). First approximations of the corresponding solar fields are shown in Table 1 and preliminary solar array layouts are shown in Figures 4 .

Table 1: First pass size estimates of the solar arrays

Parameter	*Lab. model (solar collector)*	*Field model (solar collector)*	*Units*
Output power	0.5	10	kW
ORC mean efficiency	12	12	%
Solar mean efficiency	42.5	42.5	%
Input power	9.80	196.08	kW
Durban insolation kWh/m^2/day	4.328	4.328	
Incident area	27	545	m^2
Solar collector area	3.04	3.04	m^2
No. of solar collectors	9	179	

3. Mathematical modelling

Mathematical models of the plant systems have been developed and simulated on the EES (Engineering Equation Solver) platform. Fourteen candidate working fluids and three cycle configurations have been analysed with the models. The analyses include a logic model selector through which an optimal conversion cycle configuration and working fluid mix is established.

3.1 First pass mathematical modelling (Situmbeko, 2011)

The first pass model gives an initial insight into the performance of the proposed energy conversion system design. This first pass model output together with the more detailed specifications of components for the proposed system design will yield a more detailed model with more realistic performance parameters that can now be incorporated in the design, development and validation of the physical model. In this work a more generalized model is first proposed as in Figure 6. This is then further customized to the thermo-physical properties of the different proposed working fluids. In particular a mathematical logic model is incorporated to assign an appropriate cycle configuration to each proposed working fluid.

The first pass model makes a number of assumptions such as:

- pumping and expansion efficiencies are assumed as hpump = 0.65, hturbine = 0.85
- modelling of heat exchangers at this stage is only performed as a thermal process to determine required input thermal energy and required exhaust thermal energy (detailed heat exchanger modelling will be done at a later stage)
- thermal losses in the cycle components and ducting are negligible;
- pressure head losses in the heat exchangers are negligible; and
- no work and no heat transfer occur in the valves, etc.

Three types of models can be identified with low temperature thermal cycles depending on the nature of the working fluid. Based on the fluids' T-s (temperature versus entropy) saturation curves these three types of energy conversion systems are: the conventional Rankine cycle, Rankine cycle with a recuperator and Rankine cycle with a superheater as shown in Figure 7. A summary of results of computer simulations of the first pass model is shown in Table 2.

3.2 Detailed component models: Solar field collector modelling

Detail modelling of a solar collector requires knowledge of the geometrical measurements and thermal

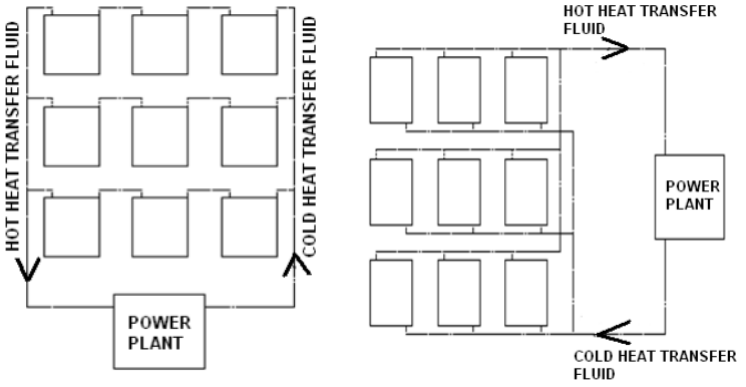

Figure 4: Two layouts options for 500 Wp solar field (requires 9 solar collectors with two layout options)

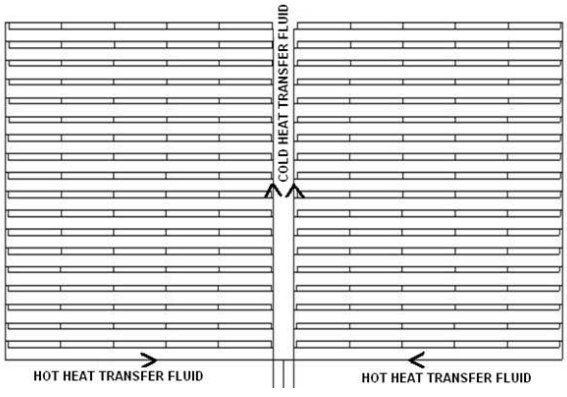

Figure 5: Possible layout for 10kWp solar field (requires 180 solar collectors)

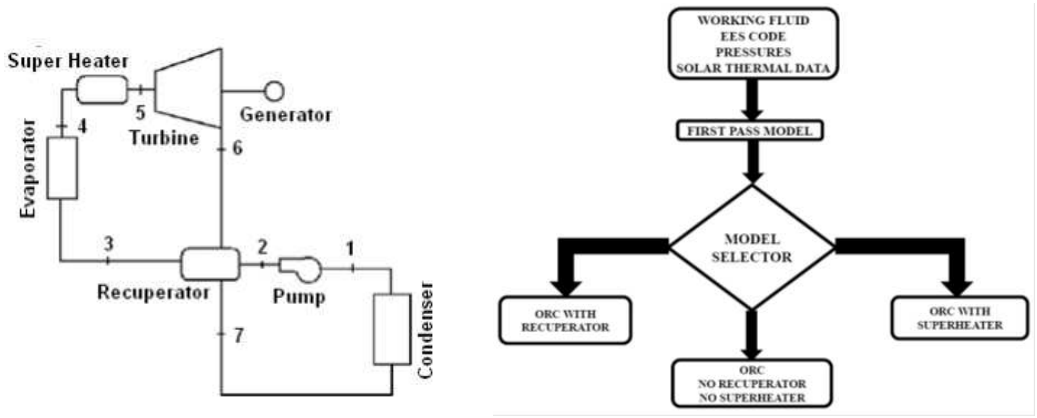

Figure 6: General configuration of a LTSTE technology and a Model Logic Selector

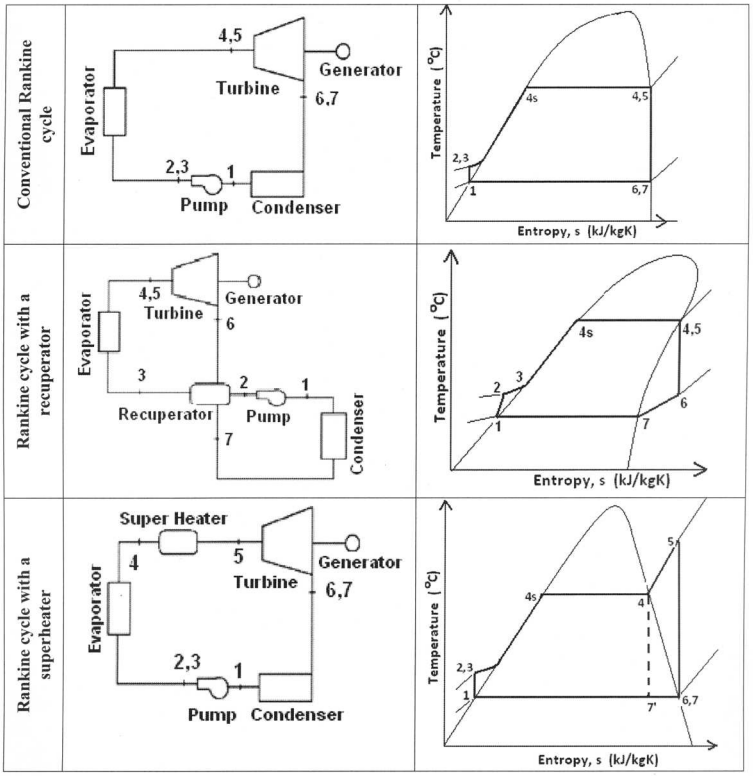

Figure 7: Three configuration options

properties of materials used in the construction. The process is based on carrying out an energy balance which can be either steady state or transient. A transient model is more useful when the solar data can be measured and fed synchronously to the simulation model.

Figure 8 shows the cross-section of a One-Riser-Pipe Solar Thermal Collector that was used to develop the energy balance represented in equations 2 to 6 below.

For the glass cover:

$$Q_{store,C} = Qin,C - Q_{conu,C\to a} - Q_{rad,C\to a} + Q_{conu,A\to C} + Q_{rad,A\to C} \quad (2)$$

For the absorber plate:

$$Q_{store,A} = Qin,A - Q_{conu,A\to C} - Q_{rad,A\to C} - Q_{cond,A\to F} - Q_{cond,A\to a} \quad (3)$$

For the heat transfer fluid:

$$Q_{cond,A\to F} = Q_{cond,F\to a} + Cth \quad (4)$$

For the storage tank:

$$Q_{store,T} = Qth - Q_{cond,T\to a} \quad (5)$$

Thermal efficiency:

$$\eta_{th} = \frac{\int Q_{th}dt}{A_c \int Gdt} \quad (6)$$

Table 2. Thermal efficiencies of different Organic Rankine Cycle configurations and different working fluids

Model type	*Working fluid*	*Q_dot_ r evaporato*	*Q_dot_ recuperator*	*Q_dot_ superheater*	*Power*	*eta_ therm*
		(kW)	(kW)	(kW)	(kW)	(%)
Rankine with recuperator no superheater	n-pentane	4.07	0.40	0	0.50	12.04
Conventional Rankine no recuperator no superheater	Benzene	4.68	0	0	0.53	11.11
Conventional rankine no recuperator no superheater	n-butane	4.56	0	0	0.54	11.60
Rankine with recuperator no superheater	n-hexane	3.75	0.61	0	0.46	12.10
Conventional Rankine no recuperator no superheater	Isobutene	4.31	0	0	0.52	11.72
Conventional Rankine no recuperator no superheater	R141b	2.60	0	0	0.30	11.30
Rankine with recuperator no superheater	Is pentane	3.90	0.38	0	0.49	12.20
Conventional Rankine no recuperator no superheater	R245fa	2.30	0	0	0.24	10.38
Rankine with recuperator no superheater	R113	1.64	0.16	0	0.20	11.89
Conventional Rankine no recuperator no superheater	R123	2.02	0	0	0.23	11.02
Rankine with superheater no recuperator	R22	2.50	0	0.21	0.33	12.01
Rankine with recuperator no superheater	Toluene	4.09	0.45	0	0.49	11.75
Rankine with superheater no recuperator	R134a	2.41	0	0.08	0.28	10.99
Rankine with superheater no recuperator	Water	23.29	0	2.57	2.80	10.81

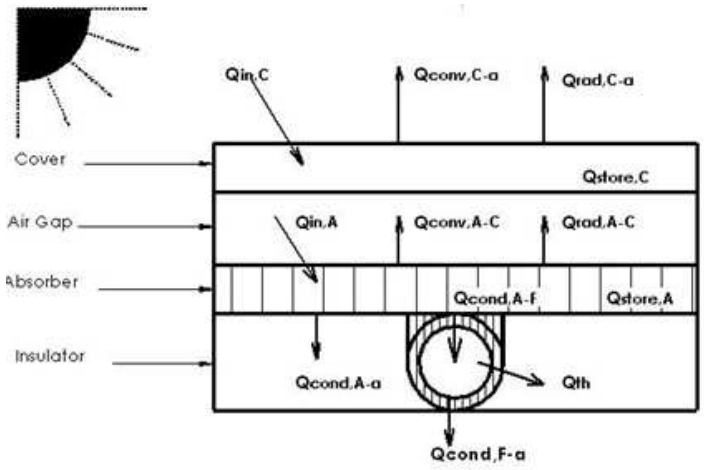

Figure 8: One pipe solar collector model

For the air gap the correlation used to determine the convective heat transfer coefficient is that given by Hollands et al (Duffie, 1991); for inclined parallel plates with a tilt angle of 0–75° which is given as:

$$Nu = 1 + 1.44\left[1 - \frac{1708(sin\ 1.8\beta)^{1.6}}{Racos\beta}\right]\left[1 - \frac{1708}{Ra\cos\beta}\right]^{+} + \left[\left(\frac{Ra\cos\beta}{5830}\right)^{1/3} - 1\right]^{+} \quad (7)$$

where the meaning of the + exponent is that only positive values of the terms in the square brackets are to be used (i.e., use zero if the term is negative); and the Nusselt number Nu and the Rayleigh number Ra are given by:

$$Nu = \frac{hL}{k} \text{ and } Ra = \frac{g\beta'\Delta TL^3}{\nu\alpha} \quad (8)$$

where:
h = heat transfer coefficient,
L = plate spacing
k = thermal conductivity

g = gravitational constant
β = volumetric coefficient of expansion (for an ideal gas, β=1/T)
ΔT = temperature difference between plates
ν = kinematic viscosity
α = thermal diffusivity

For laminar flow in circular pipes the correlation used is that given by Incropera (2007):

$$Nu_D \equiv \frac{hD}{k} = 4.36 \quad (9)$$
$$for\ uniform\ surface\ heat\ flux$$

$$Nu_D \equiv \frac{hD}{k} = 3.66 \quad (10)$$
$$forconstant\ surface\ temperature$$

For this case the transfer to the heat transfer fluid lies in between the two conditions and therefore the Nusselt number used is the average of the two.

For the Wind Convection Coefficients, Duffie (1991) recommend using:

$$h_W = \max[5, \frac{8.6V^{0.6}}{L^{0.4}}] \quad (11)$$

where V (m/s) is wind speed and L (m) is the cube root of the house volume.

The average hourly radiation can be estimated from the total daily radiation by using the following equation (Silva, 2011):

$$I = Hr_t \quad (12)$$

The coefficient to convert total daily radiation, H (Wh/m^2-day) to average hourly radiation I (W/m^2) is given by:

$$r_t = \frac{\pi}{24}(a + bcosw)\frac{cosw - cosw_s}{sinw_s - \frac{\pi w_s}{180}cosw_s} \quad (13)$$

where w is the hour angle and W_s is the sunset hour angle in degrees. The coefficients a and b are given by:

$$a = 0.409 + 0.5016\sin(w_s - 60)$$
$$b = 0.6609 - 0.4767sin(w_s - 60) \quad (14)$$

The model also requires inputs of ambient temperatures; these are included in Table 3.

Transient conditions
Considering the steady-state model above, corresponding transient models can be developed. These are however not used in the current model as the transiency is modelled into the time step segmented model.

Table 3: Hourly ambient temperatures for the modelled day (www.weather.com)

Time	*Temp. (°C)*	*Time*	*Temp. (°C)*	*Time*	*Temp. (°C)*
5am	20	1pm	26	9pm	23
6am	20	2pm	27	10pm	22
7am	20	3pm	26	11pm	21
8am	20	4pm	26	12am	21
9am	22	5pm	26	1am	21
10am	23	6pm	24	2am	20
11am	25	7pm	24	3am	20
12pm	25	8pm	23	4am	20

Storage model
The thermal storage model consists of an energy balance consisting of charging, discharging and thermal losses. In this model, however, only charging has been considered. The discharging and thermal losses will be considered at the time of coupling the solar cycle sub-model to the thermal conversion cycle sub-model. The charging model is given by the equations:

$$\dot{Q}_{tank} = \dot{m}_{wg} * Cp_{wg} * \left(T_{wg,out,30} - T_{tank}\right)$$

$$\dot{Q}_{tank} = m_{wg,tank} * Cp_{wg} * \left[\frac{T_{tank} - T_{wg,in,1}}{t_{cycle}}\right] \quad (15)$$

where:
$\dot{Q}_{tank}$ (J/s) is the heat transfer rate to the thermal storage;
$\dot{m}_{wg}$ (kg/s) is the mass flow rate of the water ethylene glycol working fluid;
$m_{wg,tank}$ (kg) is the mass of the water ethylene glycol in the storage tank;
Cp_{wg} (J/kg-K) is the specific heat capacity of the water ethylene glycol;
t_{cycle} (s) is the cycle time for the current cycle;
$T_{wg,out,30}$ (°C) is the temperature of the working fluid exiting the collector model and entering the storage tank for the current cycle;
$T_{wg,in,1}$ (°C) is the temperature of the working fluid entering the collector model at the previous cycle (it is also the temperature of the storage tank at previous cycle); and
T_{tank} (°C) is the new storage tank temperature for the current cycle.

4 Computer simulations

4.1 Description of the computer model

The model consists of a code written in EES. EES has the advantage that apart from its flexible solver capabilities it also already contains thermodynamic properties of most working fluids and materials including the ethylene glycol water mixture used in this model and the air contained in the air gap. The thermodynamic properties include density, specific

heat, thermal conductivity, viscosity, etc.

The code is arranged in the following format:

- Main Program: Calls the two procedures NusseltNumber and HourCycle; and outputs thermal storage data.
- SubProgram SegmentedModel: calculates the energy balance for each cycle; calls the I_sol
- Function I_sol: calculates the hour solar radiation
- Procedure NusseltNumber: calculates the Nusselt number for each segment of the air gap.
- Procedure HourCycle: compiles energy data for all cycles in each hour

4.2 Model validation

The model was run for the selected hourly ambient temperatures of the typical March-April day as in Table 3. The model calculated the hourly total radiation as in equations 12 to 14. Two tests were done for the 9-solar-collectors field and the 180-solar-collectors field. The model used was a one pipe model; thus it was assumed for the 9 solar collectors that three one-pipe solar collectors were connected in series and for the 180 solar collectors that eighteen one-pipe solar collectors were connected in series. The geometrical sizes and thermal properties of the single riser pipe solar collectors model are given in Table 4.

5. Results of computer models and simulations

The results of the solar model computer simulations are presented in the following charts:

5.1 Computer solar radiation model

Figure 9 shows the computed hour radiation values. The computed solar radiation is highest at noon and is almost symmetrically reducing to zero on sides, the forenoon and the afternoon. The peak at noon is 613.2 W/m^2. The simplified model seems adequate for design purposes. In actual situations the model would have to take into account other weather parameters such as cloud cover, wind and precipitation. The solar radiation curve closely follows the fourth order polynomial:

$$y = 0.296x^4 - 8.306x^3 + 59.70x^2 - 21.82x - 27.03$$

5.2 Temperature modelling results

Figure 10 shows the temperature profiles along the segments of the collectors. T_p is the temperature profile for the absorber plate and T_wg is the temperature profile for the water ethylene glycol working fluid. The numbers enclosed in the parentheses represent the number of the one-pipe-model collectors as they are connected in series. These results are for a one cycle pass with no storage model connected.

Figure 11 shows the energy profiles along the segments of the collectors. Q_dot_wg is the heat transfer profile to the working fluid and Q_dot_loss represents the thermal losses from the collector at each segment. Similarly these results are for a one cycle pass with no storage model connected.

The rate of heat gain by the working fluid decreases along linear segments of the collector whilst the rate of heat losses from the collector increases along the linear segments of the collector.

Figure 12 shows results for the 180-solar collector single pipe field model. The computer model consists of 18 one-pipe models connected in series to represent the 180-solar collector field.

There is a steady build-up of temperature for all components along the model segments and banks.

Table 4: Description of the simulated model

Length of absorber plate	2.0 m for entire collector; 200mm for each segment model
Width of absorber plate	1.0m for entire collector; 125mm for the one-pipe model
Diameter of riser pipe	6mm internal diameter
Material of absorber plate	1mm Aluminium plate
Material of riser pipe	I.D 6mmX1mm Copper Pipe
Material of insulation	40mm Polyurethane Form
Material of transparent cover	4mm Solar Grade Glass
Transmissivity of cover	0.9
Absorptance of absorber	0.9
Emissivity of absorber	0.1
Emissivity of glass	0.85
Heat transfer fluid	Ethylene glycol water; 50% concentration
Number of thermal model segments	10 for each collector; the model collector consists of a one-pipe absorber plate 2.0m length X 125mm width
Size of storage tank	300 litres for the 9 solar collectors (i.e. for the entire solar field); or 12.5 litres for one-pipe model

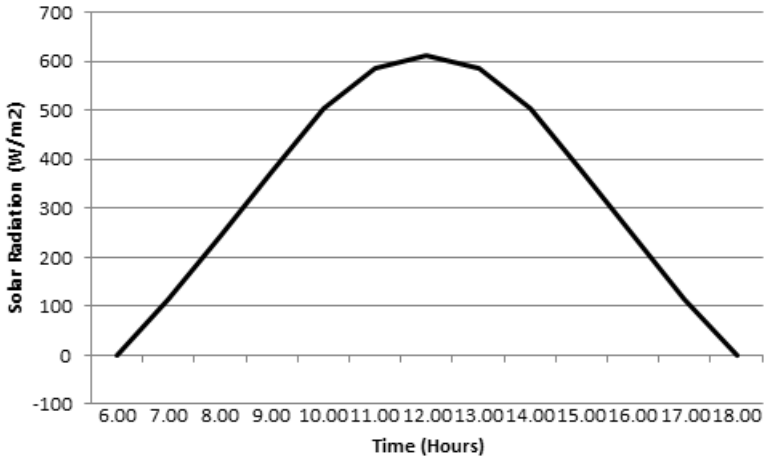

Figure 9: Simulated hourly solar radiation values

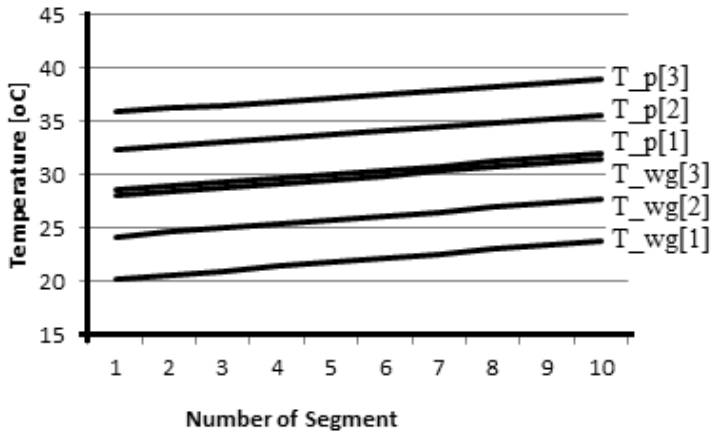

Figure 10: Plot of temperature profiles versus segment numbers

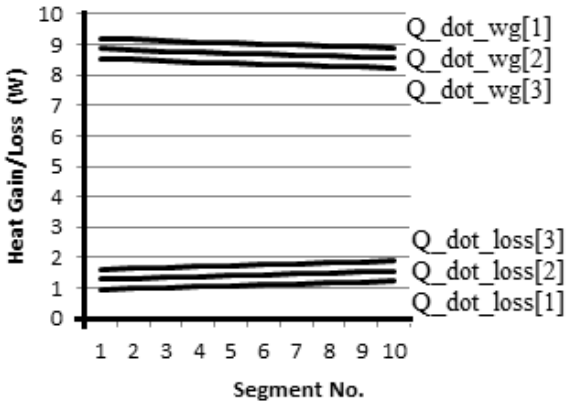

Figure 11: Energy gains and losses profiles versus segments

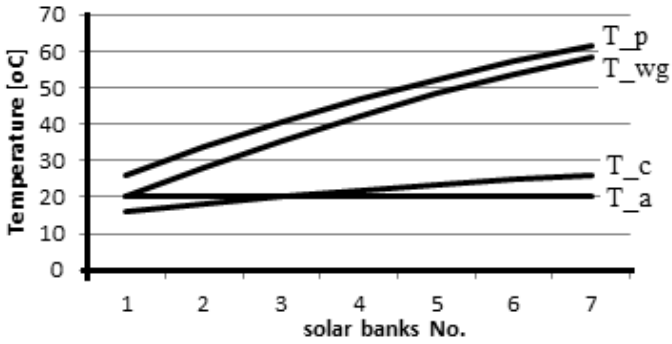

Figure 12: Temperature profile along solar banks; 180-collector model

The temperature is highest in the absorber plate and lowest in the transparent cover; also the rate of temperature increase is lowest in the transparent cover. The rate of temperature increase closely follows the same profile in both the absorber and in the working fluid.

Curve fit results yielded the following second order polynomials:

$$T\_p: y = -0.320x^2 + 8.483x + 17.93$$

$$T\_wg: y = -0.334x^2 + 9.080x + 11.32$$

$$T\_c: y = -0.087x^2 + 2.367x + 13.87$$

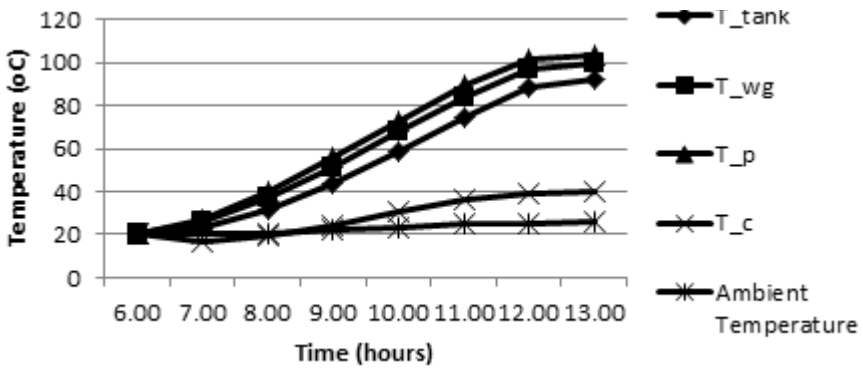

Figure 13: Hourly temperature profiles

Figure 13 shows the hourly temperature profiles. These simulations consists of several cycles (114 cycles calculated) to make an hour. The temperature measurement is taken at the end of the hour. These simulations include a thermal storage represented by the tank temperature T_tank.

The absorber plate attains the highest temperature followed by the working fluid (water ethylene glycol) at the exit of the solar field and in the tank storage. The three temperature profiles follow each other closely and build-up slowly from morning to a high about noon. The absorber increases temperature from ambient temperature of 20°C to slightly over 100°C about noon; the water ethylene glycol attains a maximum of slightly below 100°C and about 90°C at the exit of the solar collector and in the storage tank respectively. This is desirable for heat transfer to continue flowing from the absorber to the working fluid.

The transparent cover has a much lower temperature ranging from ambient temperature to about 40°C. This ensures lower thermal losses.

Curve fitting gave the following results:

$T\_p: y = -0.460x^3 + 6.007x^2 - 8.466x + 23.20$

$T\_wg: y = -0.439x^3 + 5.955x^2 - 10.06x + 24.93$

$T\_tank: y = -0.403x^3 + 5.831x^2 - 12.62x + 27.75$

$T\_c: y = -0.258x^3 + 3.694x^2 - 11.48x + 27.65$

$T\_ambient: y = 0.988x + 18.17$

5.3 Energy modelling results

Figures 14 and 15 show useful heat gains and thermal losses.

The levels of heat transfer to the working fluid in the storage tank increases with time from the lowest values in the morning (7am) to the highest values in mid-morning (11am) and then decreases with time attaining lower values at noon and 1pm respectively.

The levels of heat transfer also decrease within each hour, being higher at the beginning of the hour than at the end; this, however, could be due to the hourly radiation level being assumed constant.

The level of thermal losses increases with time from the lowest at the start of the modelling time (7am) to the highest and the end of the modelling time (1pm). Sky losses are the highest ranging from about 50% to 100%.

Figure 16 shows average hourly thermal efficiency. The thermal efficiencies are highest near the commencement of the modelling period (7am, 8am and 9am are highest; the lowest efficiencies are at 1pm followed by 12pm).

The average efficiency has a high of 56% at 8pm and a low of 35% at 1pm; the regression analysis yielded the following curve fit:

$$y = 0.055x^3 - 1.321x^2 + 4.265x + 51.42.$$

6. Discussions and conclusions

Preliminary small-scale concept plants, 500Wp and 10kWp, have been presented, modelled and computer-simulated. The first pass modelling used 14 candidate organic fluids and three optional plant configurations which gave thermal efficiencies ranging from 10.38% to 12.20%; the highest being Isopentane and organic Rankine with recuperator and the lowest being R245fa with conventional organic Rankine cycle.

The solar field modelling has been done with Ethylene Glycol Water (50% concentration) as the heat transfer fluid. The model included simulations of hourly solar insolation values, and solar collector and storage tank energy balances.

The general trend exhibited by the temperature profiles for the absorber, ethylene glycol water and transparent cover along the flow direction of the heat transfer fluid is that of a second order polynomial continuously increasing but with a diminishing gradient.

The hourly temperature profiles for the absorber, transparent cover, heat transfer fluid at

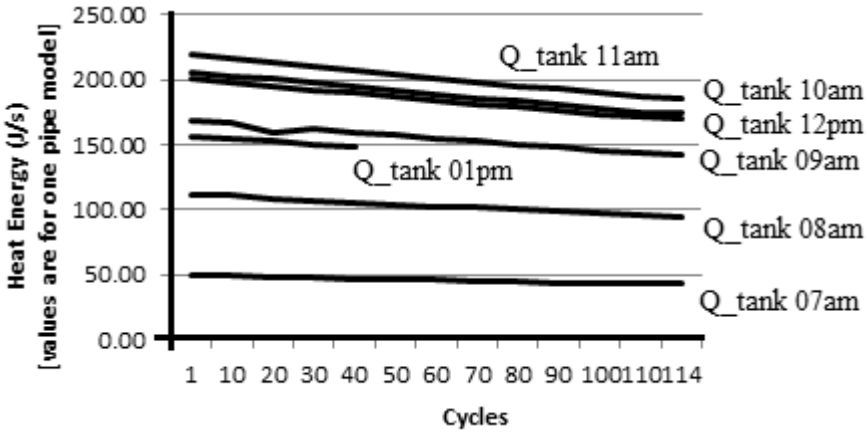

Figure 14: Heat energy rates for storage

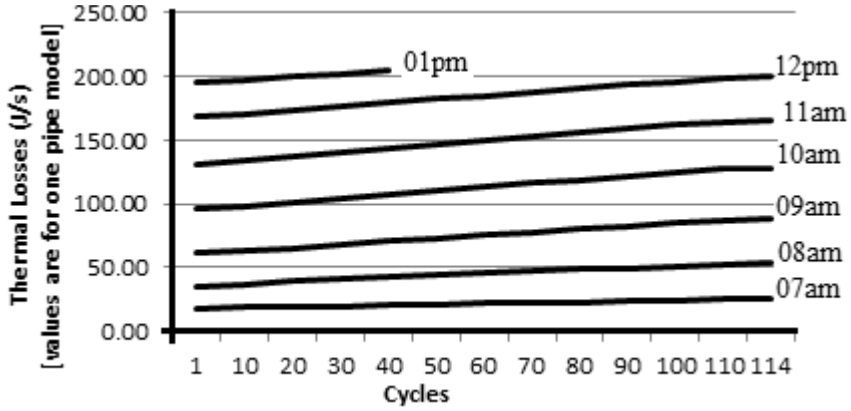

Figure 15: Thermal losses

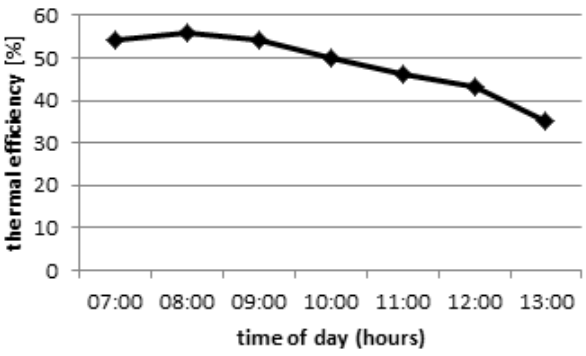

Figure 16: Average hourly thermal efficiency

collector exit, and heat transfer fluid in the storage tank, on the other hand exhibited a third order polynomial character starting with a lower gradient, developing into a steep gradient and then slowing down to a lower gradient.

The hourly efficiency curve also exhibited a third order polynomial profile starting with higher values and tailing down to lower values.

By regression one is able to mathematically determine the totals and averages for futures analyses.

A simple analysis of the 9-collector model shows the thermal energy output being less than the approximated requirements. These will be adjusted in the full simulations once the models of the other components have been finalised.

The main limitation in the simulations was the lower number of permissible variables of the academic commercial version of the software and the low computing speed to the extent that some simulation cycles had to be broken down to allow for manual entering of data midway through the simulations.

The valuable insights gained from these simulations will provide a solid basis for the final concepts designs and physical validations.

References

Duffie J.A., and Beckman W.A., (1991). Solar Engineering of Thermal Processes, 2nd Ed., John Wiley & Son, USA, p281.

Engineering Equation Solver (EES).

Groenendaal B.J., (2002). ECN project number 7.7372: Solar Thermal Power Technologies.

Incropera F.P. et al, (2007) Fundamentals of Heat and Mass Transfer; John Wiley & Sons, USA.

Nishith B. D. and Santanu B., (2009). Process integration of organic Rankine cycle, Energy Journal, Vol. 34 pp 1674–1686.

Schlaich J. and Robinson M., (1995). Principle of a

Solar Chimney: Solar Chimney, Axel Menges GmbH.
Situmbeko S. M., Inambao F. L., (2011). Mathematical Modelling and Simulation of Low Temperature Solar Thermal Energy Conversion Systems, Proceedings ISES Solar World Congress, Kassel, Germany.
Silva M R. et al, (2011). Interactive Tool to Teach Solar Parabolic Trough Concepts; Proceedings ISES, SWC, Kassel, German, September 2011.
Website:www.weather.com/weather/hourbyhour/graph/SFXX0011?begHour=2&begDay=95#hhView (accessed April 03, 2012).
Website: http://www.ienergyinc.com/(accessed November 5, 2013).
Website: www.nrel.gov/csp/troughnet/power_plant_ systems.htmlhttp://www.nrel.gov/csp/troughnet/power_plant_systems.html (accessed November 5, 2013).
Website: www.brightsourceenergy.com/technology (accessed November 5, 2013).
Website: www.:montaraventures.com/energy/wp-content/uploads/2008/05/rankine-cycle-diagram.jpg (accessed January 13, 2010).
Website: www.eng.usf.edu/~hchen4/Kalina%20Cycle.htm (accessed April 04, 2012).
Website: www.solardome.co.za/documents/file/25-solar-dome-sa-priclelist.html (accessed March 12, 2012).
Website:www.thermotechs.com/Downloads/Thermomax%20Handbook.pdf (accessed March 12, 2012).
Website: www.gaisma.com/en/location/durban.html (accessed March 12, 2012).

Received 23 May 2012; revised 4 October 2013